Characterization of the submarine disposal of a Bayer effluent (Gardanne alumina plant, southern France): II. Chemical composition of the clarified effluent and mineralogical composition of the concretions formed by its discharge in the Mediterranean Sea

Christophe Monnin, Aimée Laurenne Koumba Boussougou, Priscia Oliva, Cédric Garnier, Stéphanie Jacquet

Environmental Advances 5 (2021) 100087

Contents lists available at ScienceDirect

Environmental Advances

journal homepage: www.sciencedirect.com/journal/environmental-advances

Characterization of the submarine disposal of a Bayer effluent (Gardanne alumina plant, southern France): II. Chemical composition of the clarified effluent and mineralogical composition of the concretions formed by its discharge in the Mediterranean Sea

Christophe Monnin [a,*], Aimée Laurenne Koumba Boussougou [a], Priscia Oliva [a], Cédric Garnier [b], Stéphanie Jacquet [b]

[a] Géosciences Environnement Toulouse, CNRS - Université Paul Sabatier – IRD (Observatoire Midi-Pyrénées), 14 avenue Edouard Belin, 31400 Toulouse, France
[b] Aix Marseille Université, CNRS/INSU, Université de Toulon, IRD, Mediterranean Institute of Oceanography (MIO), UM 110, 13288 Marseille, France

ARTICLE INFO

Keywords:
Red muds
Alumina
Gardanne
Hydrotalcite
Mediterranean Sea
Bayer liquor
Bayer residue

ABSTRACT

The Gardanne alumina plant (Marseille region, Southeast France) has disposed its residues as a slurry (red muds) in the Mediterranean Sea up to 2015 when new regulations allowed the sole discharge of a clarified effluent. This reduced the quantity of suspended material from ~300 g/L to less than 10 mg/L. The detailed chemical composition of this clarified effluent has been determined by ICP-OES, ionic chromatography, 1H NMR spectroscopy and carbon analysis. It is a Na–Al–OH aqueous solution at pH 12.5 having a solute load of 1.5 g/L and an organic carbon content of about 100 mg/L, all other elements being in minor or trace amounts. A X-ray diffraction and SEM study showed that the submarine concretions forming at the outfall upon mixing the effluent with seawater are predominantly composed of a Mg–Al–OH double layer hydroxide of the hydrotalcite supergroup that contains Ca and S (wermlandite subgroup), along with minor calcite, bayerite, and rarely brucite and akaganeite (an iron hydroxide). The investigation of the stability of standard hydrotalcite in the marine environment through solubility calculations showed that hydrotalcite minerals are not stable in normal seawater and as such are prone to dissolve and release their components to the environment.

1. Introduction

The aluminum industry is the second largest worldwide after that of iron. The ore is mainly bauxite and the valued products are the aluminum oxide (alumina) and metallic aluminum produced by the reduction of alumina in energy-consuming smelters. The annual production of smelter and chemical grade alumina was over 115 million tons in 2015, largely produced using the Bayer process, i.e. the dissolution of bauxite in hot concentrated soda solutions (https://aluminiuminsider.com/red-mud-addressing-the-problem/). The production of one ton of alumina generates between 1 and 1.5 ton of bauxite residue, at a global rate of 125 million ton per year in 2013, so that the total amount of bauxite residue accumulated in the world since the beginning of the aluminum industry is over 30 billion tons (Hill and Sehnke, 2006; Mishra and Gostu, 2017).

The alumina plant located in the town of Gardanne 25 km North of Marseille (Southern France) is the last-born industrial facility in this area devoted to the production of aluminum that started at this location in 1893. It has been installed there close to the bauxite deposit of Baux-de-Provence (from which the name bauxite derives) and to a coal mine that provided the necessary energy for the process. From 1967 to the end of 2015, the Gardanne alumina plant has disposed its waste byproducts as a thickened residue (red muds) into the Mediterranean Sea through a 55 km-long pipe, 7 km of which being under water. The outfall of this pipe is at a depth of 320 m at the top of the Cassidaigne canyon which cuts the continental shelf off the coast of the Calanques National Park. Starting January 1, 2016, the slurry has been filtered to reduce the suspended material from 300 g/L to a few tens of mg/L. This produces on one hand an aqueous solution (that we designate in this work as the effluent, to distinguish it from the fluids of various compositions that circulate in the plant that may be termed Bayer liquors), and on the other hand solid residues. This clarified high-pH (12.5) effluent was still disposed at sea

* Corresponding author.
E-mail address: christophe.monnin@get.omp.eu (C. Monnin).

https://doi.org/10.1016/j.envadv.2021.100087
Received 6 July 2021; Received in revised form 22 July 2021; Accepted 22 July 2021
Available online 26 July 2021

while the solid part was stored in on-land tailing ponds at the Mangegarri site close to the plant. Mixing of the effluent with seawater formed concretions and a plume of white particles at the outfall, the size distribution, chemical composition and settling rate of which have been determined (Jacquet et al., 2021). In 2015, regulation authorities released an operating license to be renewed after five years subject to the condition that the operator (the Alteo Company) provided a way to reduce the pH of the clarified effluent and its aluminum content. This goal was achieved at the end of 2019 with the installation in the plant of a treatment unit that neutralizes the effluent by addition of CO_2 (https://alteo-environnement-gardanne.fr/). The company is also committed to studying the environmental impacts of the underwater waste disposal (Dauvin, 2010). For this sampling campaigns at sea are regularly organized. Although the case of the submarine disposal of the Gardanne Bayer effluent may be peculiar as the majority of the waste of the alumina industry is being landfilled, the disposal of the Gardanne alumina plant is a well-documented case study of industrial waste disposals at sea that need to be characterized as accurately as possible ((Morello et al., 2016; Ramirez-Llodra et al., 2015).

This work presents the chemical composition of the clarified Bayer effluent collected at the plant in December 2016. The operating conditions of the plant nowadays are not the same as those of the period at which the samples were collected, i.e. when the pH of the effluent was 12.5. We also report the mineralogical composition of the submarine concretions forming at the outfall. In order to investigate the similarities of the minerals found in the concretions to the same type material, found in pristine environments or forming because of human activities, the nomenclature of layered double hydroxides (LDH), their occurrence and conditions of formation in natural environments have been reviewed. Using available thermodynamic properties for standard hydrotalcite, we have gained insight into the stability in the marine environment, of the main mineral forming the concretions through solubility calculations.

2. Material and methods

Six samples of the liquid effluent have been directly provided by the Alteo Company in 50 ml Falcon vials. No detail about vial conditioning is available to us. These samples have been collected at the plant every day at 4 pm between December 4 and 9, 2016. This sampling procedure allows a first estimate of the variation of the effluent composition with the fluctuations of the conditions of the industrial process, at least within the restricted time span of one week (Fig. 1).

The concretions were collected at the pipe outfall at a depth of about 300 m during a cruise that took place on August 24, 2016 (see Jacquet et al.(2021) for a detailed description of the procedures at sea). These concretions have various textures, from soft to consolidated material (Fig. 3). Visual observations have guided sample collection within the concretions, taking into account features like color changes or structural aspects. Some of the concretions present fluid conduits within which several samples were taken along lines likely to reveal changes during their growth.

Jacquet et al. (2021) have sorted the samples into three groups: samples from the center (core) of the concretion belong to Group 1, Group 2 is the intermediate samples between the core and the external crust, and Group 3 is the samples taken in the external crust. There are differences in the chemical compositions from one group to the other (Jacquet et al., 2021). For the mineralogical analysis carried out in this work, each solid sample has been divided in two parts: one kept as is and the other one lyophilized. A total of 30 samples (15 raw and 15 lyophilized) have been analyzed.

2.1. Aqueous chemistry

The chemical composition of the liquid effluent was determined at the Geosciences Environnement Toulouse (GET) laboratory in Toulouse. We have measured the concentrations of Na, K, Ca, Mg, Sr, Ba, Si, Al and Fe using an ICP-OES Horiba Jobin Yvon Ultima2®. The detection limit of the ICP-OES varies form one element to the other. It is below 0.001 mmol/L for Mg, the only element selected for the analysis that could not be detected (Table 2). In parallel the concentrations of metals and of trace elements have been measured by HR-ICP-MS (ELEMENT XR, Thermo) at the Mediterranean Institute of Oceanography in Marseille

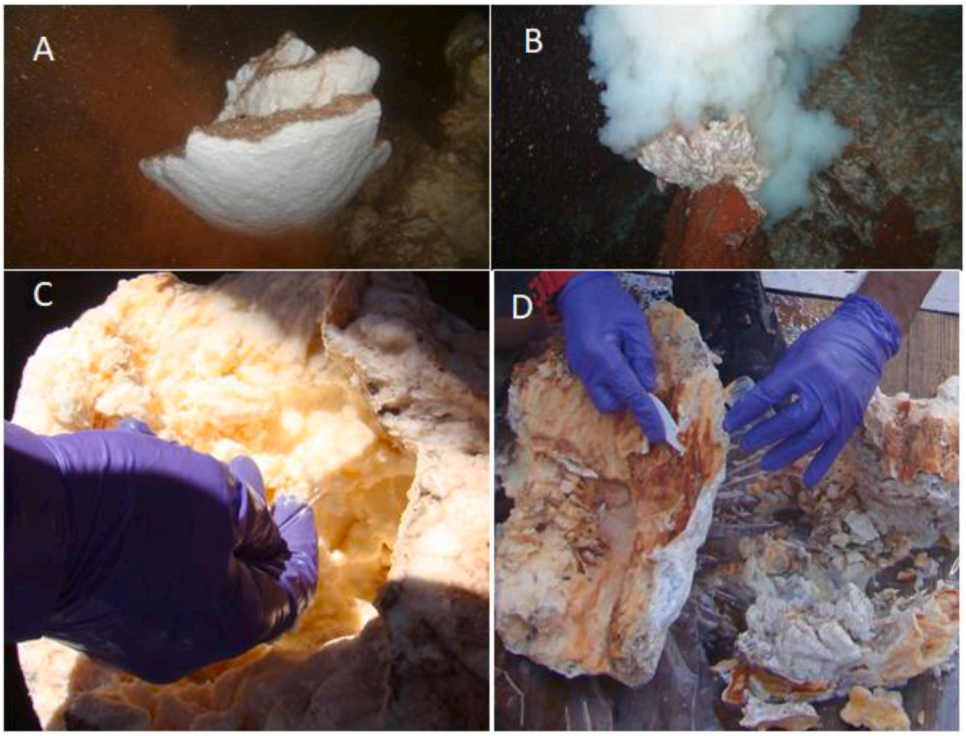

Fig. 1. In situ submarine concretions (A and B). Sampling on board the ship (C and D). See (Jacquet et al., 2021).

and is reported in a companion publication (Jacquet et al., 2021). Ionic chromatography (Dionex ICS 2000® liquid chromatographer) was used to determine the concentrations of the anions (Cl, SO_4, F, NO_2, NO_3, Br, Acetate, Formate). The Dissolved Inorganic Carbon content (DIC) and the Non Purgeable Organic Carbon content (NPOC) were measured with a Shimadzu® analyzer at the Geosciences Environnement Toulouse laboratory. In order to measure the inorganic carbon content, the analyzer acidifies the aqueous solution which is then flushed with air to purge the dissolved gases. The CO_2 released this way is analyzed by an infrared detector. In a second step the aqueous solution is combusted on a platinum catalyzer at a temperature of 680 °C and again CO_2 is analyzed. This is why the dissolved organic compound analyzed this way is termed Non Purgeable Organic carbon (see for example https://www.elgalabwater.com/blog/total-organic-carbon-toc). Volatile compounds may be lost during the purge and as such the total organic carbon content may be underestimated.

The concentrations of organic species have been determined by ^1H NMR spectroscopy at the Metatoul facility in Toulouse (www. metatoul. fr).

2.2. Mineralogical analysis

Mineralogical analyses were performed on air-dried (lyophilized) samples. Thin sections have been prepared for observations with the optical and electronic microscope and elemental analysis with the electronic microprobe. These thin sections have been polished with an ultrafine silica powder.

Powders of the concretions have been analyzed through X-ray diffraction and observed in thin sections via SEM (Scanning Electron Microscopy) at the Geosciences Environnement Toulouse laboratory. The mineralogical composition of the bulk samples was determined using random powder analysis performed on the Bruker D2 diffractometer (Cu-Kα radiation, Brag Brentano theta/theta setup, 2-80°) after crushing the total fraction in an agate mortar. In order to have a more precise analysis of hydrotalcite minerals that show variable magnitude of the basal spacing, the X-ray diffraction measurements were also made using quartz as an internal standard and were performed using D8 Advance diffractometers (Cu-Kα radiation, Brag Brentano theta/theta setup, 2-80°). The diffractograms have then been aligned on the main peak of quartz (101 at 3.34Å). Diffraction patterns of powders samples were interpreted with reference to the ICDD (pdf 2) and COD databases using the EVA software (Bruker).

We have investigated the eventual changes due to the lyophilization of the samples by comparing the X-ray diffraction patterns of raw and lyophilized samples. As no difference has been observed further analysis has been carried out on 15 lyophilized samples (Table 2), the raw material being dedicated to SEM-EDS analysis.

The electronic microprobe data (CAMECA SXFive FE) have been collected at the Centre de Caractérisation Raimond Castaing in Toulouse (http://ccarcastaing.cnrs.fr/).

3. Results

3.1. The composition of the Bayer effluent of the Alteo alumina plant in Gardanne

The chemical compositions of the 6 samples of the clarified effluent are given in Table I. The charge balance has been calculated with the PHREEQC software (Parkhurst and Appelo, 2013) along with the THERMODEMM.DAT data base of the French Geological Survey (Blanc et al., 2012) in order to assess the overall quality of the analyses.

The charge balance is the difference between the sum of the positive and negative charges in solution (expressed in equivalent.moles, i.e. the concentration in moles multiplied by the charge). This difference Δ is:

$$\Delta = \sum_c c_c.|z_c| - \sum_a c_a.|z_a| \quad (1)$$

$\sum$ is the sum of all charges in the aqueous solution:

$$\sum = \sum_c c_c.|z_c| + \sum_a c_a.|z_a| \quad (2)$$

In these expressions c is a cation and a an anion. The electroneutrality E expressed in % is:

$$E = 100\ \frac{|\Delta|}{\sum} \quad (3)$$

One can see (Table I) that the electroneutrality is about 5% except for one sample for which it is 9%, which are satisfactory values.

The Total Dissolved Solids (TDS) content is 1.5 g/L. pH is about 12.5. The major elements are Na (about 1300 mg/L or 60 mmol/L), Al (between 150 and 230 mg/L or between 5 and 9 mmol/L) and OH. Na and OH come from the soda used in the Bayer process and Al from the bauxites. All other elements are in minor concentrations (below 1 mmol/L) or below detection limit of the ICP-OES. This makes the Alteo effluent a low salinity water of the Na-Al-OH type. There is a limited, but noticeable variability of the effluent composition during the time the samples have been collected (i.e. one week). For example the Al concentration varies between 5.5 and 8.7 mmol/L, that of bromide between 7 and 129 μmol/L and that of nitrate between 4 and 265 μmol/L (Table I).

The Dissolved Inorganic Carbon content, expressed in table I in equivalent.C, is about 10 times that of normal seawater. The silica concentration is about 10 times that of seawater. Barium has a concentration similar to that of the Mediterranean sea (i.e. about 40 nmol/L; Jacquet et al., 2016). Chloride and sulfate have been detected at 2 mmol/L for Cl and 0.3 mmol/L for sulfate. Lastly the dissolved iron content is very low, about 1ppb (below 1μmol/L). Acetate and formate have noticeable concentrations, of about respectively 63 and 25 mg/L (0.94 mmol/l and 0.55 mmol/L respectively). Traces of methanol, isopropanol, lactate and succinate have been found (Table 1). The ethanol concentration (0.66 mmol/L) is comparable to that of formate. These data for organics are only indicative as no specific precaution was taken during sampling that was not originally designed for such an analysis. The Total Organic Carbon content (TOC) calculated from the sum of the organic ions and molecules is about 40% higher (in mg.C/L) than the Non Purgeable Organic Carbon (NPOC) content of the effluent (Table 1). This could reflect the bias linked to the purge during the analysis of NPOC. The organic carbon content (TOC or NPOC) is about 100 mg/L which is within the order of magnitude of waste waters (https://www.elgalabwater.com/blog/total-organic-carbon-toc).

A few compositions of Bayer liquors are reported in the literature (Couperthwaite et al., 2013; Marciano et al., 2006; Palmer and Frost, 2011). Comparison with the Gardanne clarified effluent is difficult first because of the ambiguity in the designation of the fluids themselves, as discussed in the introduction, and second because the reported compositions may correspond to fluids collected at various stages of the Bayer process in a given plant (Marciano et al., 2006). The fate of organic compounds in Bayer liquors has been given attention (Busetti et al., 2014; Power et al., 2011a; Power et al., 2011b) because of the lowering of the process yield due to the poisoning of mineral surfaces and the subsequent slowing of the nucleation and growth of alumina (Power et al., 2011a; Power et al., 2011b; Xiao et al., 2007) and of the hazard caused by hydrogen production due to the degradation of organic compounds contained in the ore (Costine et al., 2011a, 2011b). The degradation of organic matter contained in the bauxites (Busetti et al., 2014) generates amounts of oxalate that accumulate in the Bayer cycle and must be regularly purged. We have not attempted to measure the oxalate concentration in the effluent samples, but it is likely low as indicated by the rough agreement between the sum of the concentrations of organics and the directly measured DOC content of the effluent.

Table 1
Chemical composition of the six samples of the Gardanne clarified effluent collected between December 4 and 9, 2016. (*) pH measured in the GET laboratory on January 30, 2017. (**) TDS: Total Dissolved Solids. (***) Electroneutrality calculated with the PHREEQC software (see text). (****) NPOC: Non Purgeable Organic Carbon (*****) TOC: Total Organic Carbon calculated from the sum of individual concentrations of organics determined by 1H NMR spectroscopy. n.d..: not determined because of the sample volume was too small.

Sample	Date of sampling	pH (*)	Na^+ mmol/l	K^+ mmol/l	Ca^{++} mmol/l	Mg^{++} mmol/l	Sr^{++} µmol/l	Ba^{++} nmol/l	Si^{4+} µmol/l	Al^{3+} mmol/l	Fe(total) µmol/l
W16	04-12-2016	12.55	63.28	0.74	0.031	*<0.001*	2.59	41.81	37.23	8.56	0.27
W17	05-12-2016	12.53	53.31	0.60	0.028	*<0.001*	2.75	52.03	37.69	5.49	0.36
W18	06-12-2016	12.55	57.67	0.64	0.017	*<0.001*	2.22	29.16	37.49	7.13	0.36
W19	07-12-2016	12.52	53.46	0.58	0.024	*n.d.*	*n.d.*	*n.d.*	*n.d.*	6.82	*n.d.*
W20	08-12-2016	12.52	54.24	0.59	0.044	*<0.001*	1.91	27.16	34.86	6.86	0.38
W21	09-12-2016	12.51	58.41	0.65	0.081	*<0.001*	1.83	23.98	33.76	8.76	0.37
Average		*12.53*	*56.73*	*0.64*	*0.038*	*<0.001*	*2.26*	*29.02*	*36.21*	*7.27*	*0.35*

Sample	Cl^- mmol/l	SO_4^{2-} mmol/l	F^- mmol/l	Br^- µmol/L	NO_2^- µmol/L	NO_3^- µmol/L	DIC mmol.C/L	NPOC (****) mmol.C/L	NPOC mg.C/L	Electro-neutrality (***) %	TDS (**) g/L
W16	2.52	0.41	104	10	0.8	33	20.90	5.97	71.64	-5.44	1.67
W17	2.65	0.46	97	41	0.5	22	16.09	4.59	55.11	-3.34	1.44
W18	2.57	0.37	89	129	2.6	4	13.58	5.09	61.11	3.44	1.54
W19	2.95	0.47	83	57	1.7	209	14.64	5.12	61.49	-1.83	1.47
W20	3.12	0.37	62	7	4.3	144	19.52	5.17	62.03	-9.61	1.48
W21	2.88	0.39	97	12	0.2	265	12.97	5.77	69.20	4.77	1.58
Average	*2.78*	*0.41*	*89*	*43*	*2*	*113*	*16.29*	*5.29*	*63.43*	*-2.00*	*1.53*

Sample	Formate µmol/L	Ethanol µmol/L	Methanol µmol/L	Succinate µmol/L	Acetate µmol/L	Lactate µmol/L	Isopropanol µmol/L	TOC (*****) calculated mg.C/L
W16	576.7	650.3	76.1	9.0	1040.3	28.8	31.9	113.4
W17	490.6	653.3	72.4	9.0	851.1	27.4	36.1	98.6
W18	491.4	650.5	72.3	6.0	875.2	22.6	19.3	98.3
W20	463.1	665.3	75.0	9.5	849.9	25.3	32.6	95.5
W21	713.2	667.9	83.8	21.6	1073.3	48.2	87.8	134.4
Average	*547.0*	*657.5*	*75.9*	*11.0*	*938.0*	*30.5*	*41.5*	*108.1*

Extremely high concentrations of acetate (18,000 mg/L) and formate (7000 mg/L) have been reported by Cardwell and Laughton (1994) in two Bayer liquors while Xiao et al. (2007) give 4700 and 980 mg/L of acetate and 130 and 190 mg/L of formate in the effluents of two Chinese plants. Again a comparison is difficult because samples can be collected at various stages of the Bayer process, in this case before or after the oxalate purge (Marciano et al., 2006).

3.2. Mineralogical composition of the concretions formed underwater by mixing of the Bayer effluent with Mediterranean seawater

3.2.1. X-ray diffraction

The three groups of samples defined by Jacquet et al. (2021) have different mineralogical compositions (Fig. 2; Table 2). Samples from group 1 (core of the concretions) contain only hydrotalcite. Those from group 2 (intermediate samples between the core and the external crust) contain hydrotalcite and minor amounts of bayerite, calcite and akaganeite (an iron hydroxide). Brucite is observed in samples from the third group (outer part of the concretion) where the intensities of the brucite major peaks suggest that it is found in noticeable amounts. Halite likely coming from the dehydration of the sample is found in only one sample. Bayerite is an aluminum hydroxide of formula $Al(OH)_3$ named after Karl Bayer, the inventor of the Bayer process. Brucite is the magnesium hydroxide $Mg(OH)_2$. Hydrotalcite is a Mg–Al hydroxide that we describe in detail below. Akaganeite is an iron oxide that may contain some chloride and nickel.

While the hydrotalcites of groups 1 and 2 showed the same diffraction patterns, a displacement of the main hydrotalcite peak is observed for the three samples of group 3 (Fig. 2).

3.2.2. Scanning Electron Microscope and Energy Dispersive X-ray Spectroscopy (SEM/EDX)

SEM images of hydrotalcite show clusters of aggregated spherical particles (<5 µm) covered with submicrometric flakes (Fig. 3). EDX data for the "H3-soft core" sample (representative of Group 1 samples, i.e. containing only hydrotalcite) reveal that these particles contain Mg, Al and O, consistently with a hydrotalcite composition in accordance with X-ray diffraction analysis. Data for other samples show that the hydrotalcite can contain small amounts of calcium and sulfur. As no gypsum or anhydrite was detected by X-ray diffraction, Ca and S must belong to the hydrotalcite structure (Palmer and Frost, 2011; Palmer et al., 2011). Indeed, a Ca and S-containing layered double hydroxide of the hydrotalcite supergroup called wermlandite has been originally found in the county of Wermland in Sweden (Mills et al., 2012; Rius and Allmann, 1984). The only sulfur-containing compound found in hydrotalcites so far is sulfate (Mills et al., 2012) (Fig. 13).

3.2.3. Electronic microprobe

The electronic microprobe allows a more quantitative determination of the chemical composition of the analyzed crystals than SEM/EDX. Unfortunately, hydrotalcite was not stable under the beam. No reliable data could be obtained.

3.2.4. The relationship between the mineralogical and chemical compositions of the concretions

The Mg/Al ratio is a main parameter characterizing hydrotalcites. It has been calculated from their chemical composition (Jacquet et al., 2021;Table 2). Bayerite is found in Group 2 samples and brucite in Group 3 samples, so that the Mg/Al ratio of samples for these two groups is not characteristic of the sole hydrotalcites. The Mg/Al ratios of the Group 1 samples are between 1.62 and 1.80 mol/mol (Table 2).

Zhitova et al. (2016) have proposed a relationship between the ratio of the divalent and trivalent cations in LDH minerals (of the hydrotalcite and quintinite subgroups) and the measured values of the distance between the middle of two adjacent brucite layers (basal d-spacing). This distance corresponds to the principal peak in X-ray diffraction patterns at angles around 12° (2θ values of the Cu Kα radiation). Using this relationship along with the interbasal distances of the hydrotalcites lead

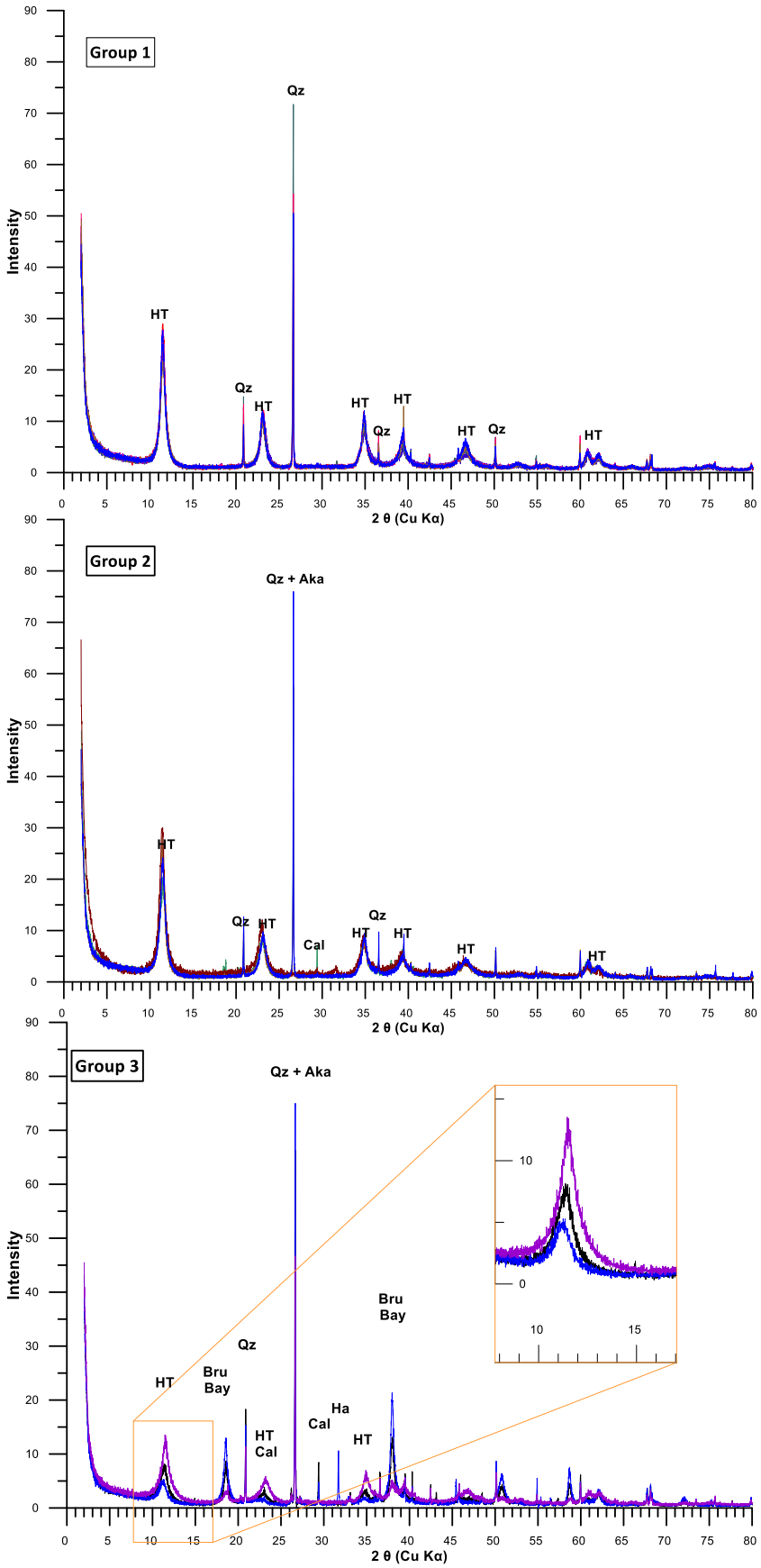

Fig. 2. X-ray diffraction diagrams showing the mineralogical assemblages observed in the 3 groups of samples. HT: Hydrotalcite; Qz: Quartz (reference material added as an internal standard); Cal: Calcite; Bru: Brucite; Bay: Bayerite; Aka: Akaganeite. The insert shows the displacement of the main hydrotalcite peak for the three samples of Group 3.

Table 2
Mineralogical and chemical (main elements) compositions of the three groups of samples. The chemical compositions are those given by Jacquet et al. (2021) converted from mg/g to mmoles/g. The Mg/Al ratio is in mol/mol.

	Sample name	Hydrotalcite	Bayerite	Calcite	Brucite	Akaganeite	Halite	Mg	Al	Ca	S	Mg/Al
Group 1	H1 soft core	+++						19.0	10.9	0.24	0.22	1.75
	H1 middle	+++						19.8	11.4	0.28	0.32	1.74
	H1 (0-2 cm)	+++						15.8	8.7	0.19	0.19	1.80
	H1 (2-4 cm)	+++						17.4	10.0	0.21	0.22	1.73
	H1 (4-6 cm)	+++						18.5	10.6	0.23	0.22	1.75
	H1 (6-8 cm)	+++						17.9	10.5	0.23	0.24	1.71
	H1 (8-10 cm)	+++						16.9	9.8	0.22	0.24	1.72
	H3 soft core	+++						20.4	12.6	0.30	0.20	1.62
Group 2	H1 (10-12 cm)	+++	+	+		+		18.3	10.6	0.27	0.29	1.73
	H1 (12-14 cm)	+++	+	+		+		13.0	7.0	0.19	0.24	1.86
	H1 (14-16 cm)	+++	+	+		+		20.2	10.5	0.24	0.40	1.93
	H3 orange vein	+++	+	+		+		18.1	9.1	0.57	0.07	1.99
Group 3	H1 external crust	++	+	+	+	+		18.6	9.5	1.07	0.36	1.96
	H2 external crust	++	+	+	+	+	+	25.7	3.1	0.72	0.22	8.26
	H3 orange vein residue	++	+	+	+	+		25.8	4.9	1.28	0.15	5.22

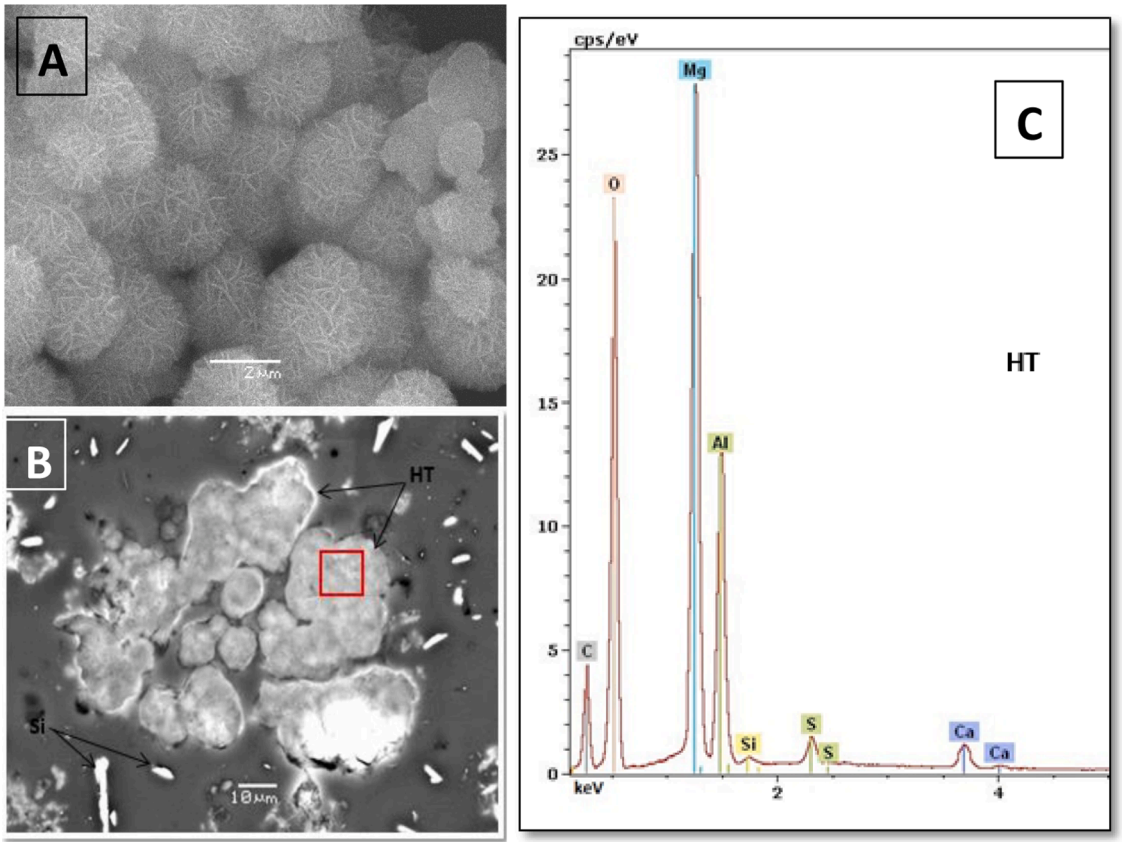

Fig. 3. A: SEM photo of hydrotalcite in the "H3 soft core" sample. B: Hydrotalcite in the "H1 soft core" sample. Note the elongated SiO_2 particles used to polish the thin sections. C: EDX spectrum of the hydrotalcite (red square in B).

to Mg/Al ratios between 2.4 and 2.8, not consistent with those estimated from the chemical analysis. The relationship proposed by Zhitova et al. may not be applicable to our samples because of differences in the composition of the hydrotalcites.

The Ca and S contents of the Group 1 samples vary within narrow ranges of 0.19–0.30 for Ca and of 0.19–0.32 mmol/g for S, for samples for Group 1 (Table 2). They are different for Groups 2 and 3 due to the presence of calcite.

To sum up, the mineralogical observations along with the chemical composition of the samples show that the main mineral found in the concretions is a layered double hydroxide (LDH) containing Ca and S (i.e. belonging to the very large hydrotalcite family). In what follows we briefly review the nomenclature of LDH in order to specify to which subgroup of the hydrotalcite supergroup the hydrotalcites forming at the outfall belong. We also review their thermodynamic properties and their presence in natural environments in order to investigate their stability in the context of the Bayer waste disposal at sea.

4. Nomenclature of layered double hydroxides and hydrotalcites

The general formula of Double Layered Hydroxides (LDH) is (Mills et al., 2012):

$$\left[M^{2+}_{1-x}M^{3+}_{x}(OH)_2\right]^{x+}\left[A^{n-}_{x/n}.mH_2O\right]^{x} \quad (4)$$

Expression in which M^{2+} is a divalent cation (e.g. Mg, Zn, Co, etc.),

M^{3+} a trivalent cation (Al, Ga, Fe, etc.), A^{n-} the exchangeable anion (CO_3^-, Cl^-, SO_4^-, etc.) and H_2O the hydration water. The LDH structure is a stacking of brucite-type layers (i.e. layers of the $Mg(OH)_2$ type) in which a divalent cation is replaced by a trivalent one. This creates an excess of positive charges in the brucite layers and thus a deficit of negative charges in the interlayer space. This deficit is compensated by the inclusion in the interlayer space of a mobile anion, the nature of which can be variable (Goh et al., 2008). This is why LDHs are also called anionic clays.

The LDH supergroup is very large and includes natural and synthetic compounds. LDHs find a lot of applications in various fields (Cavani et al., 1991; Mills et al., 2012; Theiss et al., 2016). The hydrotalcite mineral is the archetype of LDH in which the divalent cation is magnesium, the trivalent cation aluminum and the anion carbonate (Mills et al., 2012). The most currently accepted formula for hydrotalcite is $Mg_6Al_2(OH)_{16}[CO_3]\bullet 4H_2O$. This corresponds to an Mg/Al ratio of 3 (Mills et al., 2012). Nevertheless other formulas are also found for minerals also called hydrotalcites. For example (Blanc et al., 2012) call hydrotalcite a mineral with an LDH structure and a formula $Mg_4Al_2O_7.10H_2O$, without carbonate. These authors call hydrotalcite-CO_3 the mineral with carbonate. (Mills et al., 2012) place hydrotalcite-CO_3 in the LDH subgroup of quintinite with a Mg/Al ratio of 2 and not in the hydrotalcite subgroup. One can also find the wording "hydrotalcite-like minerals" (e.g. (Johnson and Glasser, 2003)) for minerals of the hydrotalcite type.

This ambiguity in the hydrotalcite formulas and naming is further enhanced by the fact that hydrotalcites are minerals of variable composition (solid solutions) and studies reporting their properties rarely use the same compounds. . For example Allada et al. (2002) have studied hydrotalcites with a Mg/Al ratio of 2.85. Zhitova et al. (2016) have quantified the rate of substitution Mg/Al in hydrotalcites of standard formula by measuring the displacement of the characteritic peaks in X-ray diffraction patterns (Vegard's law). The influence of the Mg/Al ratio on the stability of the brucite layers of hydrotalcite has also been addressed by Yang et al. (2007) in their ab initio DFT (Density Functionnal Theory) study.

To summarize, hydrotalcites can incorporate foreign cations into their structure as substituents for the divalent cation in the brucite layers or anions in the interlayer space. They can also accommodate various loosely bound anions in their interlayer space which lead to high anion exchange capacity. Their large surface area also favors adsorption (Goh et al., 2008).

5. The stability of hydrotalcite in the marine environment

5.1. Thermodynamic properties of hydrotalcite

A few studies have addressed the question of the thermodynamic properties of LDHs. Bravo-Suarez et al. (2004a, 2004b) have proposed a group contribution method (sum of components, oxides or ions) to estimate the thermodynamic properties of LDHs. These authors recommend a careful use of their estimates, especially for a quantitative analysis of LDH stability, but their method can nevertheless provide indications of the relative stability of LDHs following changes in the substituting cations.

Johnson and Glasser (2003) have calculated the hydrotalcite solubility product from solubility measurements at 25 °C. Allada et al. (2002, 2005) have measured the enthalpies and entropies of formation of Mg–Al hydrotalcites. They evidenced the more important role of the interlayer anion than that of the substituting cation in the brucite layers on the stability and exchange capacity of the minerals. Rozov et al. (2011) have measured the solubility of minerals in the hydrotalcite-pyroaurite series (pyroaurite being a hydrotalcite in which Fe replaces Al) as a function of the Fe/Al ratio. They have extracted the thermodynamic properties of the end members (hydrotalcite and pyroaurite) and the parameters of the regular solid solution from Lippmann's diagrams. All these authors have studied hydrotalcites with different Mg/Al ratios: 2 for Johnson and Glasser (2003), 3 for Rozov et al. (2011) and 2.85 for Allada et al. (2005). This lead to large differences between reported thermodynamic parameters. Moreover the structural formulas vary from one author to the other, from formulas written with one Mg to those with 4 Mg. A detailed study (beyond the scope of the present work) is necessary to extract reference values of the hydrotalcite thermodynamic properties.

Despite these uncertainties, hydrotalcites have been included in some of the numerous thermodynamic data bases constructed to simulate the evolution of water-mineral-gas systems in various natural (geochemical) or industrial environments. For example the Thermo-Chimie data base has been elaborated by ANDRA, the French agency for the storage of nuclear wastes (Giffaut et al., 2014) while the French Geological Survey proposed the Thermoddem data base (Blanc et al., 2012). These two data bases include thermodynamic properties of standard hydrotalcite (with Mg/Al = 2) based on those of (Johnson and Glasser, 2003). They are provided in a format suited for the PHREEQC software, among others (Parkhurst and Appelo, 2013). As no thermodynamic data are available for wermlandite, we have used those for standard hydrotalcite of formula $Mg_4Al_2(OH)_{12}[CO_3]\bullet 2H_2O$ as an analogue to gain further insight into its stability in the effluent and in the marine environment.

5.2. Hydrotalcite solubility in the clarified effluent and in seawater

The ionic product Q of a standard hydrotalcite of formula $Mg_4Al_2(OH)_{12}[CO_3]\bullet 2H_2O$ is the product of the activities of the ionic components of the solid in the aqueous solution:

$$Q = a_{Mg(aq)}^{4} \cdot a_{Al(aq)}^{2} \cdot a_{OH(aq)}^{12} \cdot a_{CO3(aq)} \cdot a_{H2O(l)}^{2} \quad (5)$$

Expression in which a is the activity of the *ith* species. The saturation index Ω is defined as the logarithm of the ratio of the ionic product to the solubility product K_{sp} at a given temperature and pressure:

$$\Omega = log\left[\frac{Q}{K_{sp}}\right] \quad (6)$$

The calculation of the hydrotalcite ($Mg_4Al_2O_7.10H_2O$) and hydrotalcite-CO_3 ($Mg_4Al_2(OH)_{12}(CO_3).2H_2O$) saturation indices using the PHREEQC software along with the THERMODDEM.DAT database shows that Mediterranean seawater is undersaturated with respect to these two minerals. Because the Mg concentration of the clarified effluent could not be measured with the ICP-OES, its saturation index could not be calculated. According to the THERMODDEM.DAT data base (Blanc et al., 2012), hydrotalcite is more stable (less soluble) than hydrotalcite-CO_3.

Aluminum is at very low concentrations (below 1μg/l, less than 30 nmol/L) in the Western Mediterranean seawater (Chou and Wollast, 1997). The calculation of the hydrotalcite and hydrotalcite-CO_3 solubilities in seawater shows that increases in the Al concentration in seawater by factors of 250 and of 50, respectively, are necessary to bring hydrotalcite or hydrotalcite-CO_3 to saturation. Bringing seawater to saturation with these minerals only slightly changes its pH, with a variation of less than 0.1 pH unit.

A Mg concentration of about 10 nanomol/L is necessary to reach hydrotalcite saturation in the Gardanne clarified effluent at pH 12.5 with an aluminum content of 200 mg/L (7.3 μmol/L). A Mg concentration of 140 nanomol/L would bring the effluent at saturation with hydrotalcite (CO_3). In this latter case hydrotalcite (without CO_3) becomes supersaturated.

It can be speculated that the seawater Al concentration may be higher than that of normal seawater in areas where Al is released by the red muds (the slurry) that have been discharged until 2016. In this case the hydrotalcite stability field could be reached at distance from the outfall. Monitoring of the water column in the area impacted by the

historical red mud discharge during the planned environmental surveillance will provide further insight into the recovery of the Cassidaigne canyon from disturbance

The knowledge of the hydrotalcite stability is of high relevance for the quantification of the environmental impacts of the red mud and effluent discharge in the Mediterranean Sea due to the capacity of this mineral to scavenge metals from solution. Such equilibrium calculations give only orders of magnitude for now, due to the high variability of the hydrotalcite composition and to the uncertainties of the thermodynamic parameters.

5.3. Natural analogues

Hyperalkaline waters exist in nature, with pH values up to 12.5 (e.g. Monnin et al., 2014; Schrenk et al., 2013). They are linked to the aqueous alteration of mantellic rocks (peridotites) during which ferrous iron is oxidized to ferric and water reduced to dihydrogen and hydroxide and peridotites are transformed into serpentinites. They can be found on land in sections of the oceanic floor carried onto continents (called ophiolites) by plate tectonics or underwater in the deep ocean where peridotites come exposed to seawater. The emblematic location of these waters is the Lost City site off the Mid-Atlantic ridge south of the Azores (Kelley et al., 2001). One of the features of these waters is that they lose their magnesium and are enriched in calcium by the serpentinization process. When they discharge into their environment, they mix with local waters, either continental or marine, leading to the formation of concretions as high as the 60-m high pinnacles of Lost City (Kelley et al., 2001) or the Aiguille de Prony in the Southern lagoon of New Caledonia (Monnin et al., 2014). In the mixing zone, Mg provided by the local waters (river of sea) reacts with the hydroxide ion to form brucite. Concretions analyzed at the venting sites of these hyperalkaline springs are composed of brucite and Ca-carbonates. In some places the aluminum content of the waters is high enough for hydrotalcite to form (Chavagnac et al., 2013; Ludwig et al., 2006).

The acetate and formate contents of the Alteo effluent (respectively of 600 and 300 μmol/L, or 30 and 15 mg/L) are larger by factors of 3 and 60 than those of the high pH fluids venting in the deep Atlantic ocean at the Lost City site, which has already been termed elevated (Lang et al., 2010). These high organic compound contents are able to sustain the development of adapted microorganisms (Postec et al., 2015; Quemeneur et al., 2014) that may participate to mineral formation as shown at Lost City (Lang et al., 2010; Lang et al., 2012) and in the alkaline hydrothermal system of Prony Bay in New Caledonia (Monnin et al., 2014; Pisapia et al., 2017).

There is a clear analogy of these natural springs with the submarine discharge of the Gardanne effluent. On one hand, mixing of a high pH water and of an Mg-rich water leads to the formation of brucite. On the other hand, mixing of the Al–OH-rich effluent with Mg-rich seawater leads to the formation of hydrotalcite, which is a form of substituted brucite. Brucite is stable only at high pH (Monnin et al., 2014). The analysis of precipitates collected in alkaline springs in Oman at different pH values shows the progressive disappearance of brucite when pH decreases (Chavagnac et al., 2013).

Environmental conditions leading to a pH decrease will tend to destabilize hydroxides such as hydrotalcite. There is nevertheless one example in nature where a hydrotalcite-like compound is stable at pH values close to neutrality. This is the peculiar case of the Eve Verda waters (Aosta Valley, Italy) where mixing of a Cu-rich acidic mine water with a perennial spring leads to the dramatic and colorful formation of an Al–Cu hydrotalcite-like compound (Tumiati et al., 2008). Although an extreme case, this example shows that element substitution in the brucite layers and the nature of the cations can affect the stability of an LDH up to the point where it becomes stable at near-neutral conditions. The Gardanne clarified effluent contains trace metals that can be incorporated in the hydrotalcite structure thus modifying its stability. It nevertheless seems that because of the very peculiar conditions of the disposal of the Bayer effluent in the sea the hydrotalcites formed at the outfall may present a unique composition, although their compositions indicate that they are related to the wermlandite group.

A unique case of hydrotalcite authigenesis has been described in polluted sediments of a lagoon in the Virgin Islands (Stoffyn et al., 1977). Hydrotalcite may be preserved in the marine environment at locations of hypersedimentation rates such as those created by alumina refinery waste disposal (Alongi and McKinnon, 2011). A study of hydrotalcite preservation in these very peculiar environments would require a complete description of the hydrological and sedimentological conditions of the dumping sites. Hydrotalcite has also been shown to form right below the ship when waste from an Al refinery was dumped into the North Sea from a barge, but no trace of it was found is the local sediments (Vandelannoote et al., 1987). This later point provides another example of the instability of hydrotalcite in the marine environment.

5.4. The interaction between red muds and seawater

The treatment of red muds by seawater (Burke et al., 2013; Couperthwaite et al., 2013; Hanahan et al., 2004; Palmer and Frost, 2011) has been studied especially for the case of alumina plants located close to the sea shore, like in Australia. These authors have studied the treatment of red muds by seawater for their neutralization and for their disposal in tailing ponds and not in the marine environment. This technical solution is not feasible for the Gardanne plant for technical and economic reasons, mainly linked to land use in a densely populated area (Bru et al., 2014). Because the liquid part of the red muds is in fact the clarified effluent, common features between these studies and the present work are observed. For example Couperthwaite et al. (2013) have found that the addition of seawater to red muds leads to the formation of a "Bayer precipitate" mainly composed of hydrotalcite and calcium carbonate. Burke et al. (2013) report results of an experiment during which 100 ml of a Bayer effluent is mixed with 200 ml of seawater. The newly formed minerals are hydrotalcite, calcite and aragonite, with traces of gypsum. Palmer and Frost (2011) have conducted the same experiment, but with a seawater/effluent volumetric ratio of 4.5. The minerals forming this way are again hydrotalcite, calcite and aragonite, but with traces of halite that likely come from some process concentrating the aqueous solution, due to the very high solubility of halite.

The newly formed minerals found in the mineralogical assemblages described in these examples of the treatment of red muds by seawater or by mixing the liquid effluent with seawater are the same as those found at the outfall of the clarified effluent of the Gardanne plant. Differences come from the solid part of the red muds that contain the minerals residual of the original bauxites, like iron oxides, or those formed during the Bayer process, like cancrinite and sodalite.

6. Conclusions

The submarine discharge of a high pH clarified Bayer effluent of the Gardanne alumina plant in the Mediterranean Sea has lead to the massive formation of concretions at the outfall. These concretions are mainly composed of hydrotalcite, a Mg–Al Double Layered Hydroxide than contains small amounts of Ca and S and as such likely belongs to the wermlandite group. Samples taken in the inner part of the concretions are solely composed of hydrotalcite. Those taken in the external crust and thus closest to seawater have a noticeable content of brucite. Minor amounts of calcite, bayerite and akaganeite are found in these samples and in those intermediate from the crust and the inner part of the concretions. The aluminum and hydroxide necessary for the formation of hydrotalcite are brought by the Na–Al–OH effluent while magnesium comes from seawater. As such hydrotalcite massively forms in a zone where these two waters mix. The calculation of hydrotalcite solubility in the two endmembers shows that they are undersaturated with respect to this mineral, on the effluent side because of the absence of magnesium

and on the seawater side because of the low pH and low aluminum concentration. This means that on the long run these massive concretions at the outfall will disappear (hydrotalcite will dissolve) when the discharge of the effluent stops.

The solubility calculations also show that an increase of the aluminum content of seawater could allow to reach the hydrotalcite stability filed. This may happen at the seafloor if aluminum is locally released by the red muds that have been discharged in the Cassidaigne canyon for more than 50 years. As such a hydrotalcite particle formed at the outfall and transported from it by the plume to a distant sediment covered with red muds could find an environment where it will be preserved. This scenario supposes that the red muds release aluminum to the water column, which still has to be studied.

Because of the high capacity of hydrotalcite to scavenge metallic ions from solution either by crystallographic substitution, interlayer intercalation and/or surface adsorption, it will play a major role in releasing these metals to the marine environment if it is destabilized when the discharge of the high pH Bayer effluent of the Gardanne alumina stops. This metal release to the marine environment will eventually lead to the formation of secondary minerals like insoluble oxides, but this requires a detailed investigation to be proven.

Declaration of Competing Interest

The authors declare that they have no known competing financial interests or personal relationships that could have appeared to influence the work reported in this paper.

Acknowledgments

This work has been carried out within the framework of a contract between the ALTEO Company and the Mediterranean Institute of Oceanography (Université Aix-Marseille and CNRS), with the Geosciences Environnement Toulouse laboratory as a sub-contractor. We gratefully acknowledge the logistical and financial support provided by ALTEO and the CREOCEAN consulting firm. We are thankful to the captain and crew of the R/V Janus of the COMEX Company, and to the Calanques National Park. All the material contained in the present study reflects the authors' observations and findings. Many thanks also to the technicians and engineers of Geosciences Environnement Toulouse (chemical analyses: P. Besson and C. Causserand; X-rays: Michel Thibaud, Ludovic Menjot and Frédéric Candaudap; SEM: Thierry Aigouy; thin sections: Fabienne de Parseval) for their efficient services.

Our colleague and co-author Cédric Garnier, who had played key roles in the elaboration and advancement of this project has passed away during this work. May he rest in peace.

References

Allada, R.K., Navrotsky, A., Berbeco, H.T., Casey, W.H., 2002. Thermochemistry and aqueous solubilities of hydrotalcite-like solids. Science 296 (5568), 721–723.

Allada, R.k., Navrotsky, A., Boerio-Goates, J., 2005. Thermochemistry of hydrotalcite-like phases in the MgO–Al_2O_3–CO_2–H_2O system: a determination of enthalpy, entropy, and free energy. Am. Miner. 90 (2-3), 329–335.

Alongi, D.M., McKinnon, A.D., 2011. Impact of hydrotalcite deposition on biogeochemical processes in a shallow tropical bay. Mar. Environ. Res. 71 (2), 111–121.

Blanc, P., et al., 2012. Thermoddem: a geochemical database focused on low temperature water/rock interactions and waste materials. Appl. Geochem. 27 (10), 2107–2116.

Bravo-Suarez, J.J., Paez-Mozo, E.A., Oyama, S.T., 2004a. Models for the estimation of thermodynamic properties of layered double hydroxides: application to the study of their anion exchange characteristics. Quimica Nova 27 (4), 574–581.

Bravo-Suarez, J.J., Paez-Mozo, E.A., Oyama, S.T., 2004b. Review of the synthesis of layered double hydroxides: a thermodynamic approach. Quimica Nova 27 (4), 601–614.

Bru, K., d'Hugues, P., Michel, P., Save, M., 2014. Usine d'alumines de Spécialités d'ALTEO Gardanne (13). Tierce Expertise sur le Dossier de Demande d'Autorisation d'Exploiter (DDAE) Visant à Supprimer les Rejets de boues Rouges en Maintenant un rejet d'effluent Liquide Résiduel. Rapport final. BRGM/RP-64161-FR.

Burke, I.T., et al., 2013. Behavior of aluminum, arsenic, and vanadium during the neutralization of red mud leachate by HCl, gypsum, or seawater. Environ. Sci. Technol. 47 (12), 6527–6535.

Busetti, F., et al., 2014. Physicochemical characterization of organic matter in bayer liquor. Ind. Eng. Chem. Res. 53 (15), 6544–6553.

Cardwell, T.J., Laughton, W.R., 1994. Analysis of fluoride, acetate and formate in Bayer liquors by ion chromatography. J. Chromatography A 678 (2), 364–369.

Cavani, F., Trifirò, F., Vaccari, A., 1991. Hydrotalcite-type anionic clays: preparation, properties and applications. Catal. Today 11 (2), 173–301.

Chavagnac, V., et al., 2013. Mineralogical assemblages forming at hyper-alkaline warm springs hosted on ultramafic rocks: a case study of Oman and Ligurian ophiolites. Geochem., Geophys., Geosyst. 14 (7), 2474–2495.

Chou, L., Wollast, R., 1997. Biogeochemical behavior and mass balance of dissolved aluminum in the western Mediterranean Sea. Deep Sea Res. Part II: Top. Stud. Oceanogr. 44 (3), 741–768.

Costine, A., Loh, J.S.C., Power, G., 2011a. Understanding hydrogen in bayer process emissions. 2. Hydrogen production during the degradation of unsaturated carboxylic acids in sodium hydroxide solutions. Ind. Eng. Chem. Res. 50 (22), 12334–12342.

Costine, A., Loh, J.S.C., Power, G., Schibeci, M., McDonald, R.G., 2011b. Understanding hydrogen in Bayer process emissions. 1. Hydrogen production during the degradation of hydroxycarboxylic acids in sodium hydroxide solutions. Ind. Eng. Chem. Res. 50 (22), 12324–12333.

Couperthwaite, S.J., et al., 2013. Bauxite residue neutralisation precipitate stability in acidic environments. Environ. Chem. 10 (6), 455–464.

Dauvin, J.C., 2010. Towards an impact assessment of bauxite red mud waste on the knowledge of the structure and functions of bathyal ecosystems: the example of the Cassidaigne canyon (north-western Mediterranean Sea). Mar. Pollut. Bull. 60 (2), 197–206.

Giffaut, E., et al., 2014. Andra thermodynamic database for performance assessment. ThermoChim. Appl. Geochem. 49, 225–236.

Goh, K.-H., Lim, T.-T., Dong, Z., 2008. Application of layered double hydroxides for removal of oxyanions: a review. Water Res. 42 (6-7), 1343–1368.

Hanahan, C., et al., 2004. Chemistry of seawater neutralization of bauxite refinery residues (red mud). Environ. Eng. Sci. 21 (2), 125–138.

Hill, V.G., Sehnke, E.D., 2006. Bauxite. N.C.T.. In: Kogel, J.E. (Ed.), Industrial Minerals & Rocks: Commodities, Markets, and Uses. Society for Mining. Metallurgy and Exploitation Inc. - Ingelwood, pp. 227–261.

Jacquet, S., et al., 2021. Characterization of the submarine disposal of a Bayer effluent (Gardanne alumina plant, southern France): I. Size distribution, chemical composition and settling rate of particles forming at the outfall. Chemosphere 263, 127695.

Jacquet, S.H.M., Monnin, C., Riou, V., Jullion, L., Tanhua, T., 2016. A high resolution and quasi-zonal transect of dissolved Ba in the Mediterranean Sea. Mar. Chem. 178, 1–7. https://doi.org/10.1016/j.marchem.2015.12.001.

Johnson, C.A., Glasser, F.P., 2003. Hydrotalcite-like minerals ($M_2Al(OH)(6)(CO_3)(0.5).XH_2O$, where M = Mg, Zn, Co, Ni) in the environment: synthesis, characterization and thermodynamic stability. Clays Clay Min. 51 (1), 1–8.

Kelley, D.S., et al., 2001. An off-axis hydrothermal vent field near the Mid-Atlantic Ridge at 30 degrees N. Nature 412 (6843), 145–149.

Lang, S.Q., Butterfield, D.A., Schulte, M., Kelley, D.S., Lilley, M.D., 2010. Elevated concentrations of formate, acetate and dissolved organic carbon found at the Lost City hydrothermal field. Geochim. Cosmochim. Acta 74 (3), 941–952.

Lang, S.Q., et al., 2012. Microbial utilization of abiogenic carbon and hydrogen in a serpentinite-hosted system. Geochim. Cosmochim. Acta 92 (0), 82–99.

Ludwig, K.A., Kelley, D.S., Butterfield, D.A., Nelson, B.K., Fruh-Green, G., 2006. Formation and evolution of carbonate chimneys at the Lost City Hydrothermal Field. Geochim. Cosmochim. Acta 70 (14), 3625–3645.

Marciano, S., Mugnier, N., Clerin, P., Cristol, B., Moulin, P., 2006. Nanofiltration of Bayer process solutions. J. Membr. Sci. 281 (1–2), 260–267.

Mills, S.J., Christy, A.G., Genin, J.M.R., Kameda, T., Colombo, F., 2012. Nomenclature of the hydrotalcite supergroup: natural layered double hydroxides. Mineral. Mag. 76 (5), 1289–1336.

Mishra, B., Gostu, S., 2017. Materials sustainability for environment: red-mud treatment. Front. Chem. Sci. Eng. 11 (3), 483–496.

Monnin, C., et al., 2014. Fluid chemistry of the low temperature hyperalkaline hydrothermal system of Prony Bay (New Caledonia). Biogeosciences 11 (20), 5687–5706.

Morello, E.B., et al., 2016. The ecological impacts of submarine tailings placement. In: Hughes, R.N., Hughes, D.J., Smith, I.P., Dale, A.C. (Eds.), Oceanography and Marine Biology: An Annual Review, vol. 54. Oceanography and Marine Biology. Crc Press-Taylor & Francis Group, Boca Raton, pp. 315–366.

Palmer, S.J., Frost, R.L., 2011. Characterization of Bayer hydrotalcites formed from bauxite refinery residue liquor. Ind. Eng. Chem. Res. 50 (9), 5346–5351.

Palmer, S.J., Grand, L.M., Frost, R.L., 2011. The synthesis and spectroscopic characterisation of hydrotalcite formed from aluminate solutions. Spectrochim. Acta Part a-Mol. Biomol. Spectrosc. 79 (1), 156–160.

Parkhurst, D.L., Appelo, C.A.J., 2013. Description of input and examples for PHREEQC version 3-A computer program for speciation, batch-reaction, one-dimensional transport, and inverse geochemical calculations, U.S. Geol. Surv. Tech. Methods, pp. 1–497.

Pisapia, C., et al., 2017. Mineralizing Filamentous Bacteria from the Prony Bay Hydrothermal Field Give New Insights into the Functioning of Serpentinization-Based Subseafloor Ecosystems. Frontiers in Microbiology 8 (57). https://doi.org/10.3389/fmicb.2017.00057.

Postec, A., et al., 2015. Microbial diversity in a submarine carbonate edifice from the serpentinizing hydrothermal system of the Prony Bay (New Caledonia) over 6-year

period. Frontiers in Microbiology 6 (857). https://doi.org/10.3389/fmicb.2015.00857 https://doi.org/.
Power, G., Loh, J.S.C., Niemela, K., 2011a. Organic compounds in the processing of lateritic bauxites to alumina Addendum to Part 1: origins and chemistry of organics in the Bayer process. Hydrometallurgy 108 (1-2), 149–151.
Power, G., Loh, J.S.C., Wajon, J.E., Busetti, F., Joll, C., 2011b. A review of the determination of organic compounds in Bayer process liquors. Anal. Chim. Acta 689 (1), 8–21.
Quemeneur, M., et al., 2014. Spatial distribution of microbial communities in the shallow submarine alkaline hydrothermal field of the Prony Bay, New Caledonia. Environ. Microbiol. Rep. 6 (6), 665–674.
Ramirez-Llodra, E., et al., 2015. Submarine and deep-sea mine tailing placements: a review of current practices, environmental issues, natural analogs and knowledge gaps in Norway and internationally. Mar. Pollut. Bull. 97 (1–2), 13–35.
Rius, J., Allmann, R., 1984. THE superstructure of the double-layer mineral wermlandite MG7(AL0.57, FEO.433+) (OH)18 2+. (CA0.6, MG0.4) (SO4)2(H2O)12 2. Z. Kristallogr. 168 (1-4), 133–144.
Rozov, K.B., Berner, U., Kulik, D.A., Diamond, L.W., 2011. Solubility and thermodynamic properties of carbonate-bearing hydrotalcite-pyroaurite solid solutions with a 3:1 Mg/(Al+Fe) mole ratio. Clays Clay Min. 59 (3), 215–232.
Schrenk, M.O., Brazelton, W.J., Lang, S.Q., 2013. Serpentinization, carbon, and deep life. In: Hazen, R.M., Jones, A.P., Baross, J.A. (Eds.), Carbon in Earth. Reviews in Mineralogy & Geochemistry, pp. 575-606.
Stoffyn, M., Dodge, C.H., Mackenzie, F.T., 1977. Neoformation of hydrotalcite due to industrial inputs in marine-sediments. Am. Mineral. 62 (11-1), 1173–1179.
Theiss, F.L., Ayoko, G.A., Frost, R.L., 2016. Synthesis of layered double hydroxides containing Mg2+, Zn2+, Ca2+ and Al3+ layer cations by co-precipitation methods—a review. Appl. Surf. Sci. 383, 200–213.
Tumiati, S., Godard, G., Masciocchi, N., Martin, S., Monticelli, D., 2008. Environmental factors controlling the precipitation of Cu-bearing hydrotalcite-like compounds from mine waters. The case of the "Eve verda" spring (Aosta Valley, Italy). Eur. J. Mineral. 20 (1), 73–94.
Vandelannoote, R., Van't Dack, L., Van Grieken, R., 1987. Effects of alkaline aluminate waste dumping on seawater chemistry. Mar. Environ. Res. 21 (4), 275–288.
Xiao, J.B., Jiang, X.Y., Chen, X.Q., 2007. Separation and determination of organic acids and inorganic anions in Bayer liquors by ion chromatography after solid-phase extraction. J. Analyt. Chem. 62 (8), 756–760.
Yang, Z., Zhou, H., Zhang, J., Cao, W., 2007. Relationship between Al/Mg ratio and the stability of single-layer hydrotalcite. Acta Phys.-Chim. Sin. 23 (6), 795–800.
Zhitova, E.S., Krivovichev, S.V., Pekov, I.V., Yakovenchuk, V.N., Pakhomovsky, Y.A., 2016. Correlation between the d-value and the M2 +:M3 + cation ratio in Mg–Al–CO_3 layered double hydroxides. Appl. Clay Sci. 130, 2–11.